The Spectrum of Benign Esophageal Lesions: Imaging Findings

Kyung Mi Jang, MD[1]
Kyung Soo Lee, MD[1]
Soon Jin Lee, MD[1]
Eun A Kim, MD[1]
Tae Sung Kim, MD[1]
Daehee Han, MD[1]
Young Mog Shim, MD[2]

Benign esophageal lesions occur in various diseases. Barium studies are useful for the evaluation of mucosal surface lesions but provide little information about the extramucosal extent of disease. Computed tomography and magnetic resonance imaging, on the other hand, permit the assessment of wall thickness, mediastinal involvement, adjacent lymphadenopathy, and distant spread. In diseases such as fibrovascular polyps, duplication cysts, scleroderma, trauma, caustic esophagitis, hiatal hernia, esophageal diverticulum, achalasia, and paraesophageal varices, the findings of imaging studies are specific, obviating the need for further invasive diagnostic work-up. The advent of helical computed tomography and its volume data set allows the acquisition of multiplanar images, and magnetic resonance imaging is useful both for this and for tissue characterization. Thus, multiplanar cross-sectional imaging further extends the role of imaging modalities to the evaluation of benign esophageal lesions. Through an awareness of the multiplanar cross-sectional appearances of various benign esophageal lesions, the radiologist can play an important role in the detection, diagnosis, further diagnostic planning, and treatment of the diseases in which they occur.

Address reprint requests to:
Kyung Soo Lee, MD, Department of
Radiology, Samsung Medical Center,
Sungkyunkwan University School of
Medicine, 50 Ilwon-dong, Kangnam-gu,
Seoul 135-710, Korea.
Telephone: (822) 3410-2511
Fax: (822) 3410-2559
e-mail: kslee@smc.samsung.co.kr

Barium contrast studies and endoscopy are useful for the evaluation of mucosal surface lesions of the esophagus but provide little information about the extramucosal extent of disease. Computed tomography (CT) and magnetic resonance imaging (MRI), on the other hand, permit the evaluation of wall thickness, mediastinal involvement, adjacent lymphadenopathy, and distant spread. With the advent of the helical technique, CT allows the rapid acquisition of both multiplanar and transaxial images, while MRI permits multiplanar imaging with high contrast resolution. In this article, the authors describe the wide range of imaging and pathologic findings of various benign esophageal lesions.

The Anatomy and Imaging Findings of the Normal Esophagus

The esophagus is a muscular tube, 20 to 24 cm in length, that connects the pharynx to the stomach. It is composed of five layers: two muscle layers (outer longitudinal and inner circular), submucosa, muscularis mucosae, and stratified squamous epithelium which changes abruptly at the cardia of the stomach into simple columnar epithelium. There is no serosal layer. The esophagus has three segments: cervical, thoracic, and abdominal, the first of which lies anterior to the vertebrae and posterior to the trachea. Throughout its course in the posterior mediastinum, the thoracic esophagus is situated adjacent to vital structures including the trachea, vertebrae, lungs, heart, blood vessels, and lymphatics. Its upper third has an intimate relationship with the trachea, while its

lower third lies close to the aorta. The abdominal esophagus is usually 3 cm or less in length and connects with the gastroesophageal junction.

In CT imaging of the esophagus, approximately 100 – 120 mL (30 gm) of intravenous contrast material is usually injected at a rate of 2 – 3 mL/sec prior to scanning, and for opacification of the esophageal lumen, an esophageal paste (Esopho-CAT; E-Z-Em, Westburg, NT, U.S.A.) may also be ingested. The apparent thickness of the esophageal wall at CT varies according to the degree of distention, and a thickness of 3 mm or more has been considered abnormal (1). According to one study (2), however, in only 4% of normal subjects is the esophageal wall more than 5 mm thick, whereas in 42% its thickness is more than 3 mm prior to dilatation of the esophageal lumen by an effervescent agent. It seems, therefore, that 5 mm, rather than 3 mm, is an appropriate maximum normal value for esophageal wall thickness. At T1-weighted imaging, the esophagus appears as a structure of low signal intensity, contrasted by fat of high signal intensity, while T2-weighted imaging indicates that its muscular wall, which shows moderate enhancement after the injection of intravenous Gd-DTPA, is of low signal intensity.

## Benign Esophageal Tumors

Leiomyoma

Esophageal leiomyoma is the most common benign esophageal tumor, accounting for more than 50% of all such tumors. Histopathologically, it consists of intersecting bands of muscle and fibrous tissue in a well-defined capsule. About 60% of these tumors are located in the distal third of the esophagus, 30% in the middle third, and 10% in the proximal third (3). Growing slowly, a tumor usually presents grossly as a discrete submucosal mass, ranging from 2 to 8 cm in diameter. Patients with these tumors are usually asymptomatic; even where a large mass significantly indents the lumen, this may be so. Where symptoms are apparent, the most common symptom of these is dysphagia. In contrast to gastric leiomyomas, esophageal leiomyomas rarely ulcerate, and hematemesis is thus extremely rare. Esophageal leiomyomatosis is sometimes associated with Alport syndrome (4).

At chest radiography, a leiomyoma may appear as a mediastinal mass (Fig. 1A), while the mass revealed by barium studies is usually discrete and submucosal. At CT, such tumors usually appear as homogeneous soft tissue lesions (5), though differentiation from other esophageal tumors (fibromas, neurofibromas, or hemangiomas) is difficult (Fig. 1B). MRI usually depicts a submucosal mass which at T2-weighted imaging is isotense to the esophageal wall (Fig. 1C). T2-weighted images of esophageal carcinomas, on the other hand, tend to show that their signal intensity is higher than that of normal esophageal wall (5).

Fibrovascular Polyp

Fibrovascular polyps are rare benign intraluminal submucosal tumor-like lesions characterized by the development of pedunculated, intraluminal masses which in the esophagus can demonstrate enormous growth. Covered with normal mucosa and containing different amounts of fibrous, vascular, and adipose tissue (6) (Fig. 2), they almost always arise from the upper third of the esophagus, near to the cricopharyngeus. On the basis of their histolog-

A   B   C
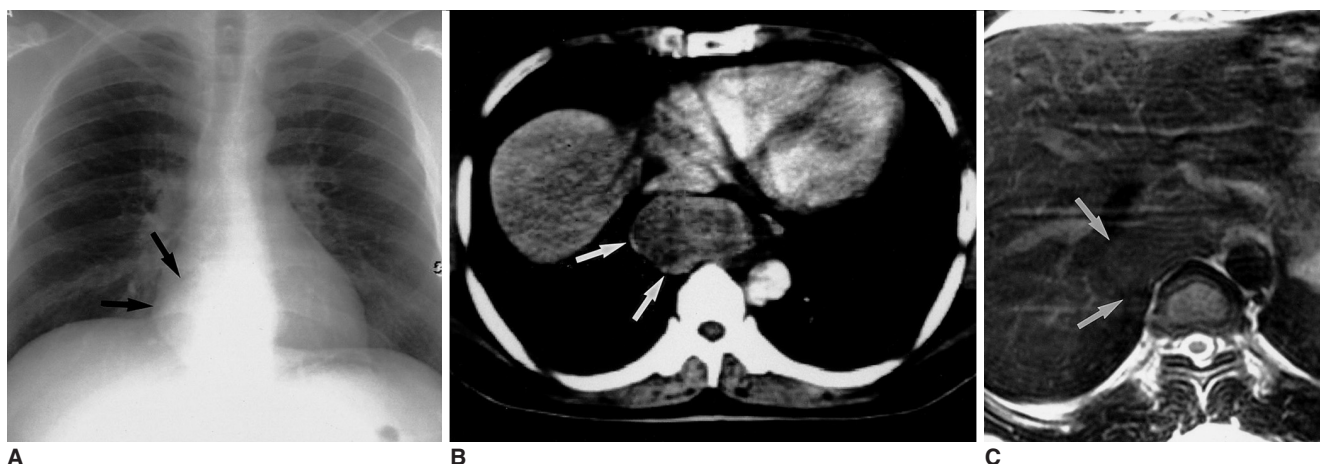
Fig. 1. Esophageal leiomyoma in a 35-year-old woman.
A. Chest radiograph shows a right retrocardiac soft-tissue mass (arrows), with obliteration of the azygoesophageal recess interface.
**B.** Enhanced (10-mm collimation) CT scan obtained at the ventricular level depicts a 60-mm-sized, slightly inhomogeneous, iso-attenuated, pear-shaped mass (arrows) in the right azygoesophageal recess.
C. T2-weighted MR image obtained at a similar level to **B** shows that compared to chest wall muscle, the mass is isointense (arrows).

ic composition, these lesions have been termed lipomas, fibromas, fibrolipomas, or fibroepithelial polyps. More recently, they have been classified as fibrovascular polyp, a term used by the World Heath Organization in their international histologic classification system. Dysphagia, vomiting, weight loss, and respiratory symptoms are the most frequent complaints of patients with fibrovascular polyps; these with long stalks, however, can regurgitate into the pharynx or mouth and cause death from asphyxiation if the larynx is occluded (7).
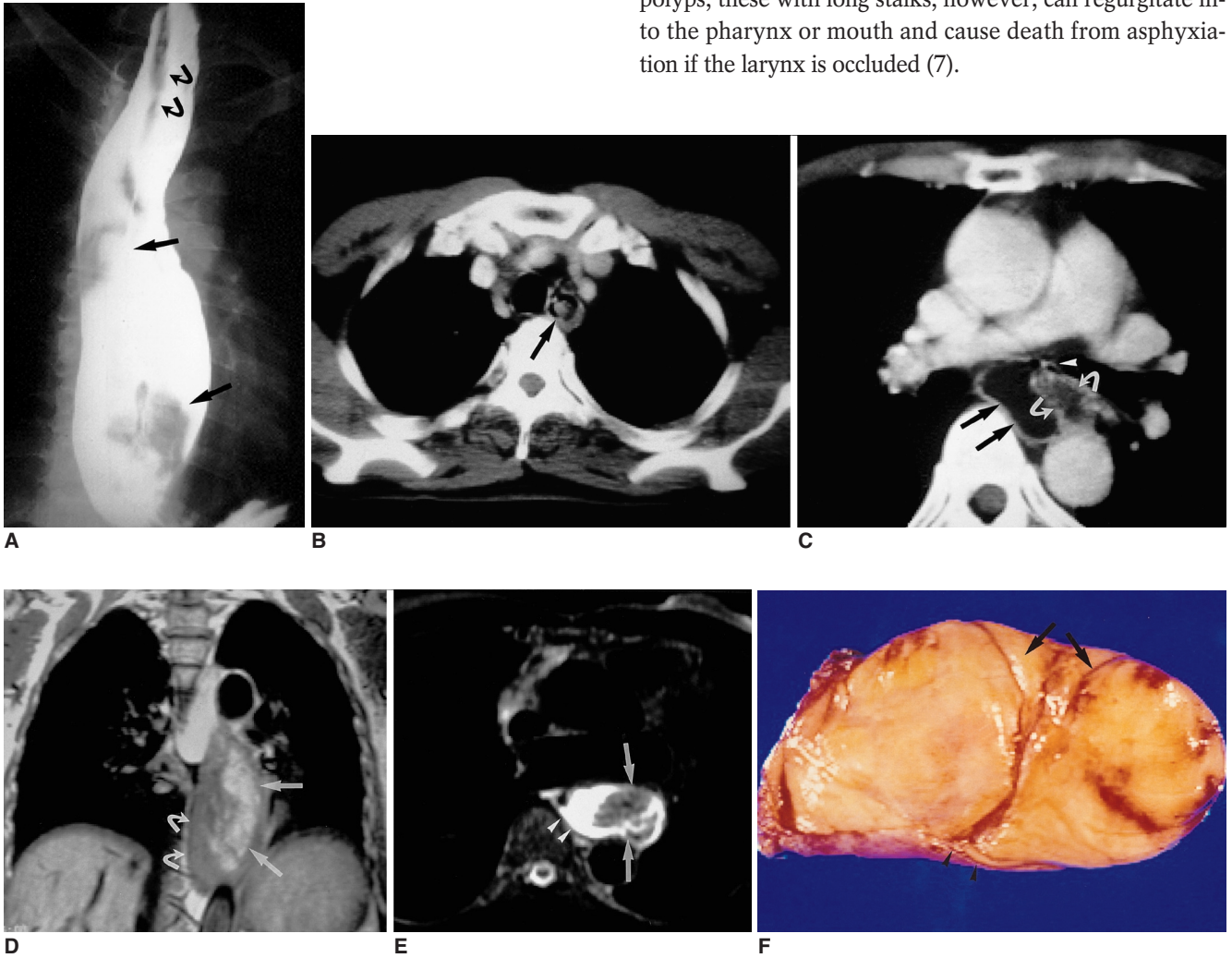
Fig. 2. Giant fibrovascular polyp in a 52-year-old man.
A. Esophagogram shows that the contrast-filled dilated esophageal lumen contains a large mass consisting of filling defects (arrows). The pedicle of the mass (curved arrows) is visible.
B. Enhanced (10-mm collimation) conventional CT scan obtained at the level of the great vessels shows a round polypoid soft-tissue lesion (arrow) arising from the posterolateral wall of the thickened esophagus. The identity of the portion, thought preoperatively to be pedicle, was confirmed at surgery.
C. CT scan obtained at the level of the distal main bronchi depicts a heterogeneous soft-tissue mass, posterior to the air-filled esophageal lumen (arrowhead). Fatty (arrows) and soft-tissue attenuation (curved arrows) is observed.
D. Coronal T1-weighted MR image reveals an elongated lesion involving the entire esophagus. Compared to chest wall muscle, it shows central high (arrows) and peripheral iso-signal intensity (curved arrows).
E. Axial T2-weighed image shows signal change in lesions compared to T1-weighted image (**D**); signal intensity is centrally low (arrows) and peripherally high (arrow heads).
F. This fragment of excised mass consists mainly of fat (arrows), and is covered with normal esophageal mucosa (arrowheads).
**G.** Photomicrograph (H & E staining, ×40) depicts intact stratified squamous epithelium (open arrows), fibrous tissue (asterisk), and numerous thin blood vessels (arrows).

Fibrovascular polyps can sometimes be identified at chest radiography by the presence of a right-sided superior mediastinal mass, anterior tracheal bowing, or both (6). The lesions usually appear at esophagography as smooth, expansile, intraluminal masses that arise in the cervical esophagus and extend into the thoracic esophagus (Fig. 2A). Although most fibrovascular polyps have a site of attachment in the cervical esophagus, barium studies often fail to demonstrate a proximal pedicle. Fibrovascular polyps containing abundant adipose tissue may appear at CT as fat-attenuated lesions that expand the lumen of the esophagus (6) (Figs. 2B, C). Polyps containing equal amounts of adipose and fibrovascular tissue may appear as heterogeneous lesions, with focal areas of fat attenuation juxtaposed with areas of soft-tissue attenuation, and those containing abundant fibrovascular tissue may appear as soft-tissue-attenuated lesions with a paucity of fat. At T1 - weighted MR imaging, fibrovascular polyps containing abundant adipose tissue are characterized by high signal intensity (8) (Fig. 2D).

Duplication Cyst

Esophageal duplication cysts account for 0.5-2.5% of all tumors or tumor-like lesions of the esophagus, and about 20% of all gastrointestinal tract duplications (9). They result from abnormal embryologic development in which
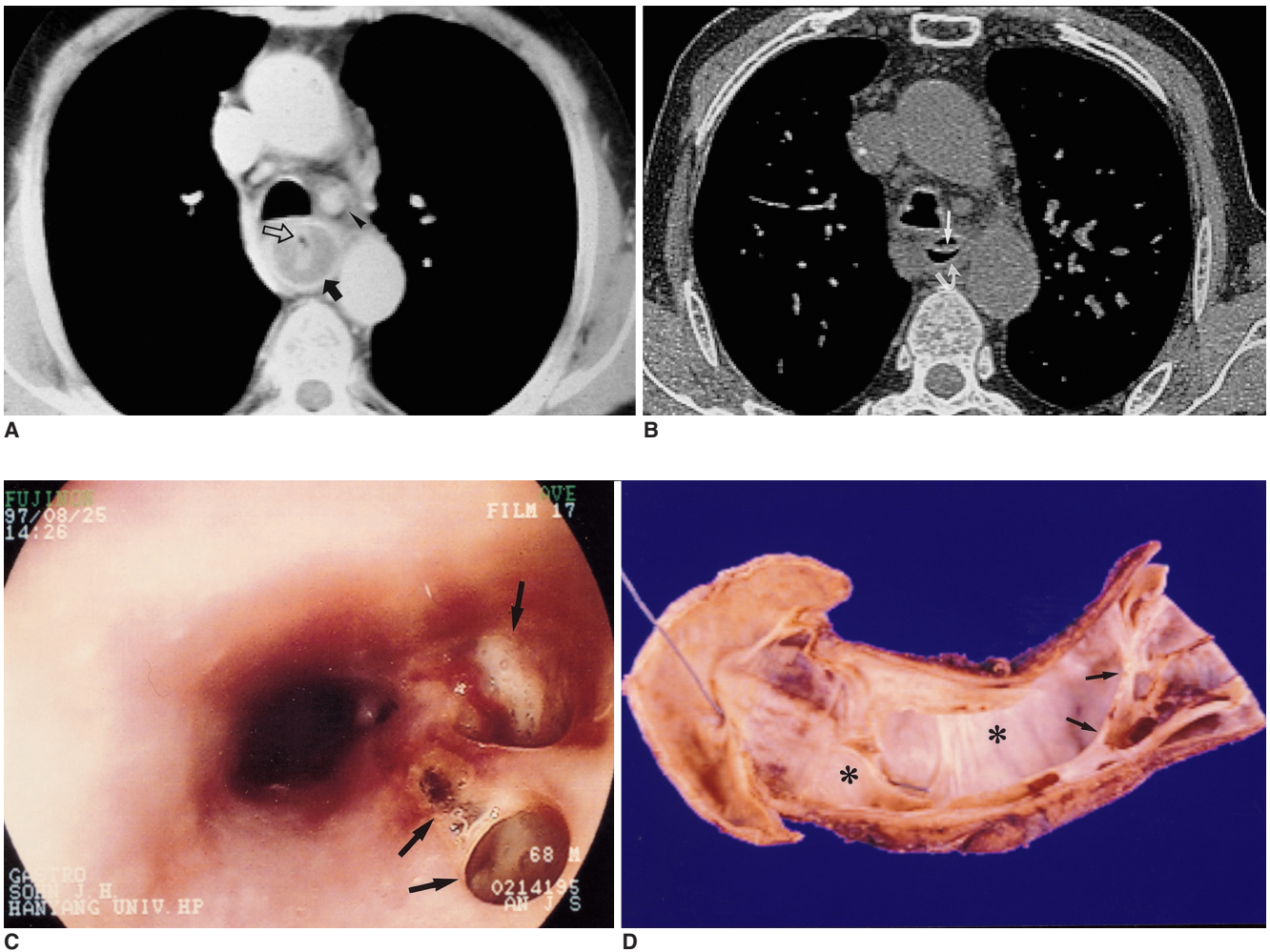
Fig. 3. A 68-year-old man with tubular esophageal duplication.
A. Mediastinal window of initial enhanced (10-mm collimation) CT scan obtained at the level of the aortopulmonary window shows two esophageal lumina : an air-filled smaller inner lumen (open arrow) is surrounded by a hematoma-filled larger outer lumen (closed arrow). A thin enhancing esophageal rim suggests the presence of mucosal lining. Also note the small lymph node in the left paratracheal area (arrowhead).
B. Follow-up thin-section (1.5-mm collimation) CT scan obtained at a similar level to (**A**) shows that the outer lumen, previously filled with hematoma, is filled with air (curved arrow). A septum (arrow) still separates the lumina.
C. Endoscopic examination reveals multiple and irregular communicating mucosal defects (arrows).
D. Pathologic specimen with a longitudinally sliced wall and septum has two lumina (asterisks) separated along their entire course by a shaggy septum with multiple defects (arrows) (reprinted, with permission, from reference 18).

nests of cells are sequestered from the primitive foregut, and may be classified as either cystic or, less commonly, tubular duplications. Although most duplication cysts are noncommunicating, tubular duplications may occasionally communicate directly with the esophageal lumen (10) (Fig. 3). Most adults with esophageal duplication cysts are asymptomatic, though symptoms caused by obstruction, bleeding, or an infected cyst may occasionally arise.

CT scans of cystic esophageal duplication depict a homogeneous mass with low attenuation and a smooth border (11) (Fig. 4). Kuhlman et al. (11) found that CT can provide information about the cystic nature, size and location of a lesion and allow the use of transesophageal needle aspiration rather than the traditional approach of surgical excision, for definitive diagnosis. CT scans of tubular duplication cysts may show two esophageal lumina, and in the esophageal wall, a thin enhancing rim, representing mucosal linings, may be apparent (10) (Fig. 3A). At T2-weighted MR imaging, duplication cysts may show bright signal intensity and a well-defined margin.

Schwannoma

Esophageal schwannoma is extremely rare; only 15 cases have been reported in the literature (12). A review of these previous reports indicates that benign schwannomas are usually located in the upper esophagus and occur more frequently in middle-aged women. A barium esophagogram reveals a large, smooth, polypoid-filled defect, and CT scans depict a mediastinal mass (Fig. 5). No distinctive characteristics differentiate these from other submucosal tumors, and at preoperative examination it is thus very difficult to distinguish between a schwannoma and other submucosal masses. Correct diagnosis requires histologic examination: positive immunohistochemical staining for S-100 protein and negative staining for smooth muscle markers such as actin and desmin confirm that the tumor originates from a nerve sheath (13).

Infectious and Inflammatory Diseases

Tuberculosis

Tuberculosis involving the esophagus usually occurs in the late stages of the disease secondary to pulmonary, mediastinal, or disseminated diseases (14). It has been suggested that CT of the mediastinum provides the most complete depiction of the tuberculous mediastinal lymphadenopathy surrounding and displacing the esophagus and the fistulous tract extending from the esophagus into the nodal mass (Fig. 6). Amorphous gas collection at enlarged mediastinal lymph nodes in patients with tuberculous lymphadenitis suggests the presence of an esophagonodal fistula (14).

4   5A   5B
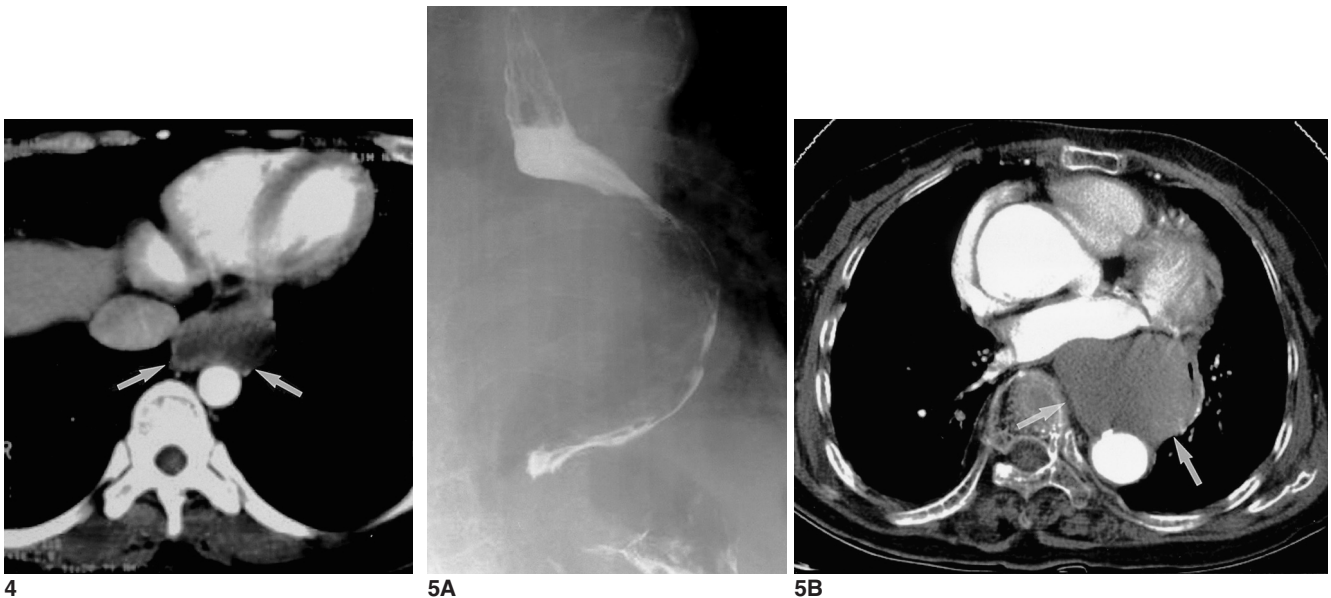
Fig. 4. A 50-year-old woman with cystic esophageal duplication. On this (7-mm collimation) CT scan obtained at the level of the liver dome, a homogeneous mass of low attenuation and with a smooth border (arrows) appears to the left of the inferior vena cava and anterior to the aorta.
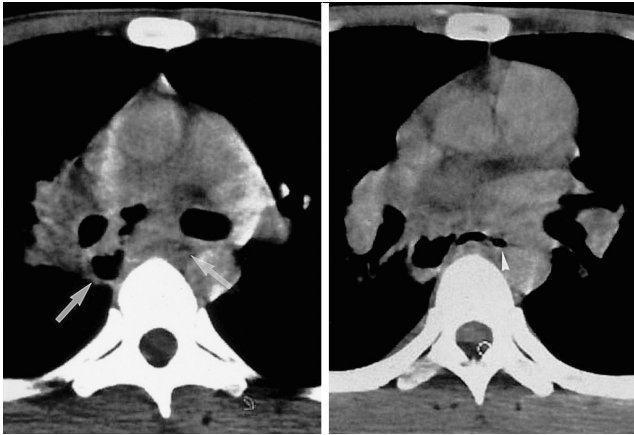
Fig. 5. Esophageal schwannoma in a 70-year-old woman.
A. Esophagogram depicts a large, smoothly elevated filling defect, and displacement of the distal esophagus.
B. Enhanced (7-mm collimation) CT scan obtained at the level of the inferior pulmonary vein shows that a homogeneous, soft-tissue lesion (arrows), of low attenuation and measuring 60 ×50 mm in diameter, occupies the left posterior mediastinum.

Candida Esophagitis

Candida esophagitis is the most common infection of the esophagus, usually occurring opportunistically in patients immunocompromised as a result of underlying malignancy; other debilitating illnesses; treatment with radiation, steroids, or cytotoxic agents; or, most recently, AIDS (15, 16). In the diagnosis of *Candida* esophagitis, double contrast esophagography shows a sensitivity of about 90%
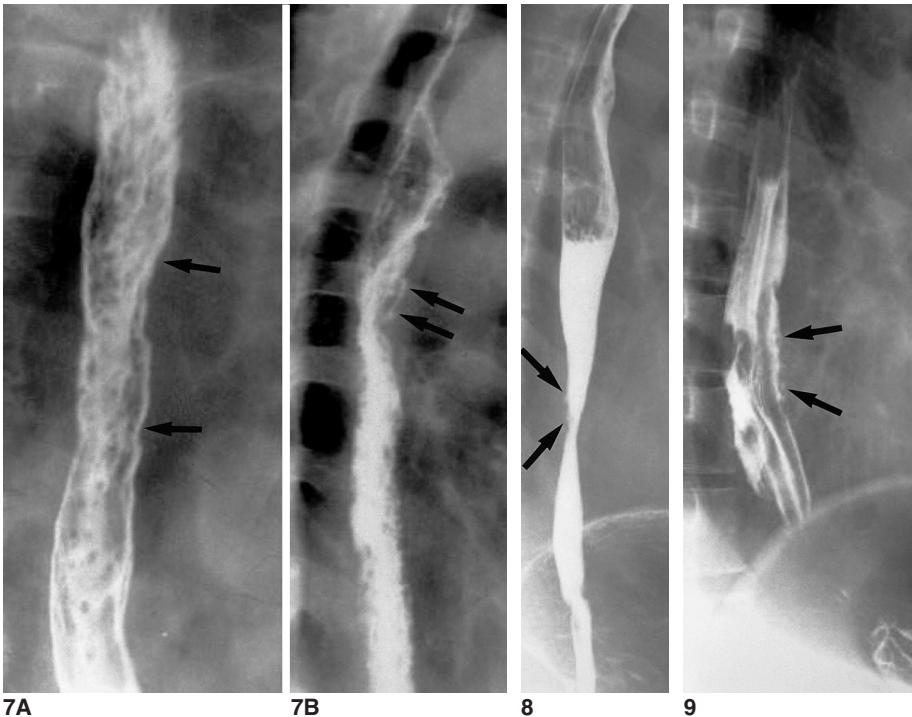
(15), demonstrating discrete plaque-like filling defects which have a finely nodular and granular, distinctive cobblestone or snakeskin-like appearance and correspond to the distinctive white plaques seen at endoscopy. These plaques consist of heaped-up areas of necrotic epithelial debris or actual colonies of *C. albicans* on the esophageal mucosa; the esophagus per se has an irregular or shaggy appearance (15, 16) (Fig. 7). The CT findings of *Candida* esophagitis, though nonspecific and commonly seen in various kinds of esophagitis, are circumferential esophageal wall thickening of more than 5 mm, with relatively long segmental involvement. Enhanced scans may also depict the target sign (circumferential wall thickening and enhancing internal mucosa) (2).

Reflux Esophagitis and Barrett's Esophagus

In the diagnosis of reflux esophagitis, the use of double-contrast esophagography has increased radiographic sensitivity to almost 90% (17). Double-contrast imaging reveals the finely nodular or granular appearance of the mucosa in the distal third or half of the thoracic esophagus, occurring due to the presence of mucosal edema and inflammation during the early stages of reflux esophagitis. As the disease progresses, double-contrast esophagography may demonstrate shallow ulcers and erosions, thickened longitudinal folds, inflammatory polyps, scarring, and strictures (18) (Fig. 8).

Barrett's esophagus involves the conversion of squamous epithelium in the distal esophagus into columnar epitheli-

A   **B**

Fig. 6. Mediastinal tuberculous lymphadenitis with esophagomediastinal fistula in a 27-year-old man with AIDS.
A, B. CT scans obtained at the levels of the left main bronchi (**A**) and the right superior segmental bronchus (**B**), respectively, reveal that within enlarged lymph nodes in the right subcarinal area, there are irregularly-shaped gas collections (arrows) that communicate with esophageal gas (arrowhead in **B**).

7A   **7B**   **8**   **9**

Fig. 7. Candida esophagitis in a 76-year-old man with diabetes mellitus.
A. Double contrast esophagogram of the proximal esophagus has a cobblestone appearance (arrows) due to the coalescence of round, ovoid, and polygonal plaques.
B. Esophagogram of the mid and distal esophagus has a shaggy appearance, and grossly irregular contour, due to the presence of multiple plaques and ulcers. Pseudomembrane (arrows) is seen as double tracts which parallel the esophagus .
Fig. 8. Reflux esophagitis in a 42-year-old woman. Double-contrast esophagogram reveals smoothly tapered luminal narrowing of the distal esophagus, and the presence of a shallow linear ulcer (arrows) .
Fig. 9. Behcet's disease in a 44-year-old man. Double-contrast esophagogram demonstrates irregular shallow ulceration within irregularly thickened folds (arrows) of the distal esophagus.

um. The most likely cause of the condition, which occurs in approximately 10% of patients with reflux disease and is premalignant with increased risk of adenocarcinoma (19), is chronic reflux esophagitis. In patients with long-segment Barrett's esophagus, the risk of developing adenocarcinoma is thought to be 30−40 times greater than among the general population (20). The characteristic radiologic feature of Barrett's esophagus is a midesophageal stricture or ulcer, often associated with a sliding hiatal hernia or gastroesophageal reflux (18, 19).

Behcet's Disease

Behcet's disease is a multi-system disorder with a clinical triad of oral and genital ulceration and ocular inflammation. The mid or distal esophagus is occasionally involved, and double contrast esophagography may reveal the presence there of discrete, superficial ulcers (21) (Fig. 9).

Scleroderma

Patients with scleroderma often develop diffuse interstitial lung disease as well as gastrointestinal symptoms such as dysphagia, regurgitation, and malabsorption. As well as revealing pulmonary parenchymal abnormalities, CT in such patients may demonstrate symptomatic esophageal dilatation and mediastinal lymph node enlargement (22) (Fig. 10).

Trauma and Caustic Esophagitis

Perforation

Perforation is the most serious and life-threatening event

to affect the esophagus : in patients with untreated thoracic esophageal perforations, the fulminant mediastinitis which occurs leads to a mortality rate of almost 100%. Endoscopic procedures are responsible for up to 75% of all esophageal perforations (23), which may also be caused by foreign bodies or penetrating trauma. Most perforation involves the cervical esophagus ; spontaneous esophageal perforation (Boerhaave syndrome) due to a sudden, rapid increase in intraluminal esophageal pressure causes full thickness perforation of normal underlying esophageal tissue, and is frequently a result of violent retching or vomiting, usually after an alcoholic binge. Patients with negative esophagograms in whom esophageal perforation is still suspected on clinical grounds may undergo CT ; in such cases,

Fig. 10. Esophageal involvement in a 59-year-old man with scleroderma. Lung window of thin-section (1-mm collimation) CT scan obtained at the level of the liver dome shows a dilated esophagus (arrows), a moderate amount of pericardial effusion (open arrows), and left pleural effusion (curved arrows). Also note the occurrence of pulmonary change consisting of irregular linear opacities, ground-glass opacities, and honeycombing.
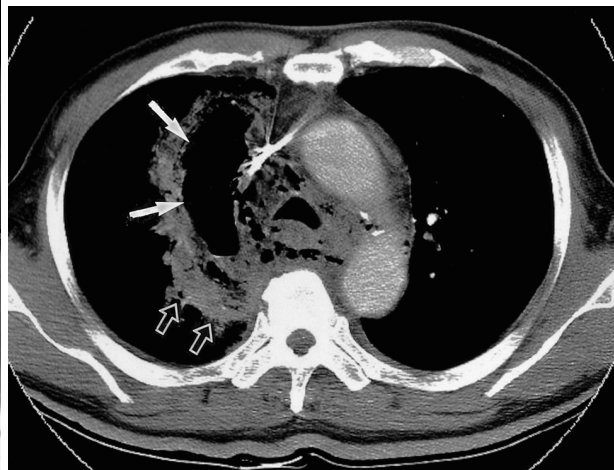
Fig. 11. Spontaneous esophageal rupture in a 58-year-old man after heavy alcohol consumption.
A. Esophagogram shows no evidence of contrast medium leakage, though mediastinal widening (arrows) is apparent . A nasogastric tube (arrowheads) was inserted.
B. Mediastinal window of enhanced (7-mm collimation) CT scan obtained at the level of the aortic arch demonstrates widening of the right superior mediastinum (arrows), and extraluminal air. Also note that parenchymal consolidation (open arrows), probably due to passive atelectasis associated with mediastinal widening, has occurred in the right upper lobe.

A　　　**B**

findings of extraluminal gas in the mediastinum are highly suggestive of esophageal perforation (Fig. 11). Where this has occurred, CT is also useful for determining the extent of extraluminal gas and fluid in the mediastinum and for monitoring patients who are treated nonsurgically (24).

Fistulae

Esophageal-airway fistula

In adults, esophageal-airway fistulae are usually acquired lesions. They may occur as complications of tumors or infections and are also caused by trauma. It has been suggested that because it is noninvasive, CT should be the modality of choice for demonstrating their presence (25) (Fig. 12). Owing to the free ingress of air from the airway to the esophagus, the precise locations and size of the communication are outlined by air contrast.

Esophagopleural fistula

Esophagopleural fistulae are usually caused by previous surgery, infection, esophageal instrumentation, radiation, or direct invasion of the pleural space by advanced esophageal carcinoma. The CT findings of esophagopleural fistula include visualization of the fistulous tract, the presence of barium, air and fluid in the pleural space, and pneumonia (26) (Fig. 13).

Caustic Esophagitis

Long, ulcerated strictures may be observed in patients who have ingested lye or other caustic agents, and in se-

vere cases, diffuse esophageal narrowing may reduce the thoracic esophagus to a thin, filiform stricture (27) (Fig. 14A). Cross-sectional images depict narrowing or obliteration of the esophageal lumen, and perifibrotic tissue may be observed (Fig. 14B). Reformatted CT images may be useful for demonstrating the surrounding fibrotic change which caustic esophagitis leads to (Fig. 14C).

Miscellaneous Diseases

Hiatal Hernia

Depending on the relationship between the cardia, the diaphragm, and the herniated portion of the stomach, hiatal hernias are classified as either sliding, accounting for about 99% of all that occur, or paraesophageal. The presence of the former is indicated if single-contrast barium studies performed with the patient in a prone position demonstrate the presence of a lower esophageal mucosal ring (web-like narrowing at the gastroesophageal junction's membranous ridge, covered superiorly by squamous epithelium and inferiorly by columnar epithelium forming the squamocolumnar junction) 2 cm or more above the diaphragmatic hiatus (Fig. 15A). Even in the absence of a definite mucosal ring, a hernia can often be recognized by the presence within it of gastric folds. In paraesophageal hernias, a portion of the stomach herniates through the esophageal hiatus into the chest alongside the distal esophagus, while the cardia retains its normal position below the diaphragm (Fig. 16). Rarely, all or most of the stomach herniates through the esophageal hiatus, producing a gas-

A **B**

Fig. 12. Esophagotracheal fistula in a 42-year-old woman with blunt trauma.
A. Mediastinal window of unenhanced (7-mm collimation) CT scan obtained at the level of the distal trachea shows a fistulous tract (arrows) between the trachea and esophagus. The superior mediastinum is widened, and there is air and soft tissue attenuation (open arrows). Also note the presence of extensive subcutaneous emphysema in the anterior chest wall.
B. Three-dimensional CT image using the shaded-surface display technique indicates that at the distal trachea, a fistulous tract (arrows) is present.

tric volvulus.

At CT scanning, a hiatal hernia may appear as a dilated distal esophagus, with or without air-fluid level in the lumen, or as displacement by the stomach of the paraesophageal line (28) (Fig. 15B).

Esophageal Diverticulum

Diverticula may be formed either by pulsion due to increased intraluminal esophageal pressure or by traction due to fibrosis in adjacent periesophageal tissue. Pulsion esophageal diverticula, which have a round contour and wide neck, consist only of mucosa, without a muscular layer. Traction diverticula, on the other hand, contain all layers of the esophageal wall, including muscle. Diverticula may be classified according to their location (29), the most common of which are the pharyngoesophageal junction (e.g. Zenker's diverticulum, pulsion type), the middle esophagus (mostly the traction type), and the distal esophagus just above the esophageal hiatus (e.g. epiphrenic diverticulum, pulsion type) (Fig. 17). Because their walls con-

A

B
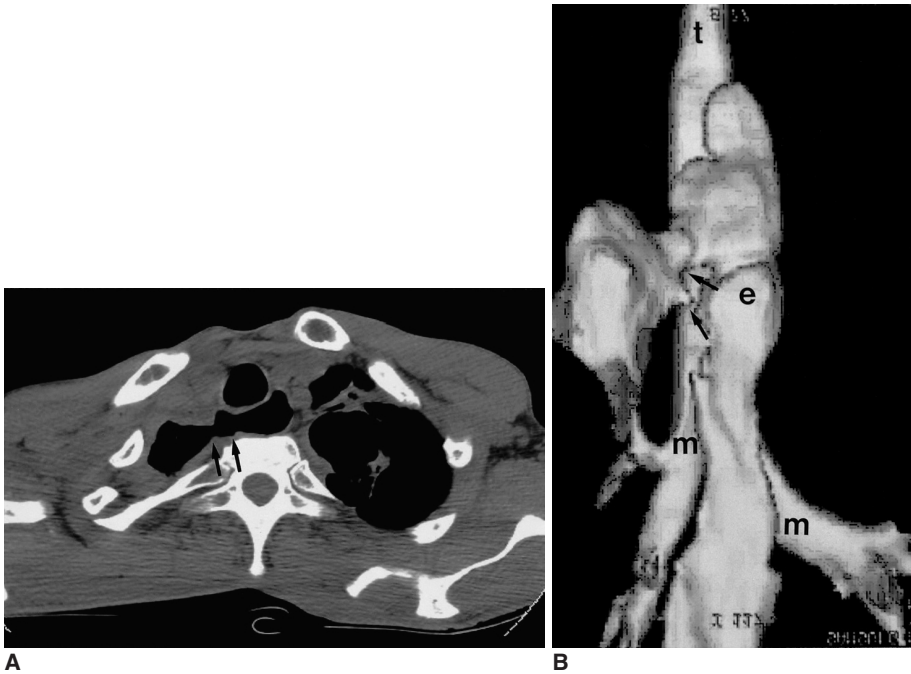
Fig. 13. Esophagopleural fistula in a 35-year-old man with chronic destructive pulmonary tuberculosis.
A. Mediastinal window of unenhanced (7-mm collimation) CT scan obtained at the level of the thoracic inlet depicts a fistulous tract (arrows) between the proximal esophagus and right pleural space.
B. Posteroanterior view of three-dimensional CT image using the shaded-surface display technique reveals the presence of fistulous tracts between the esophagus and right pleural space (arrows)(t = trachea, e = esophagus, m = main bronchus).

A

B

C
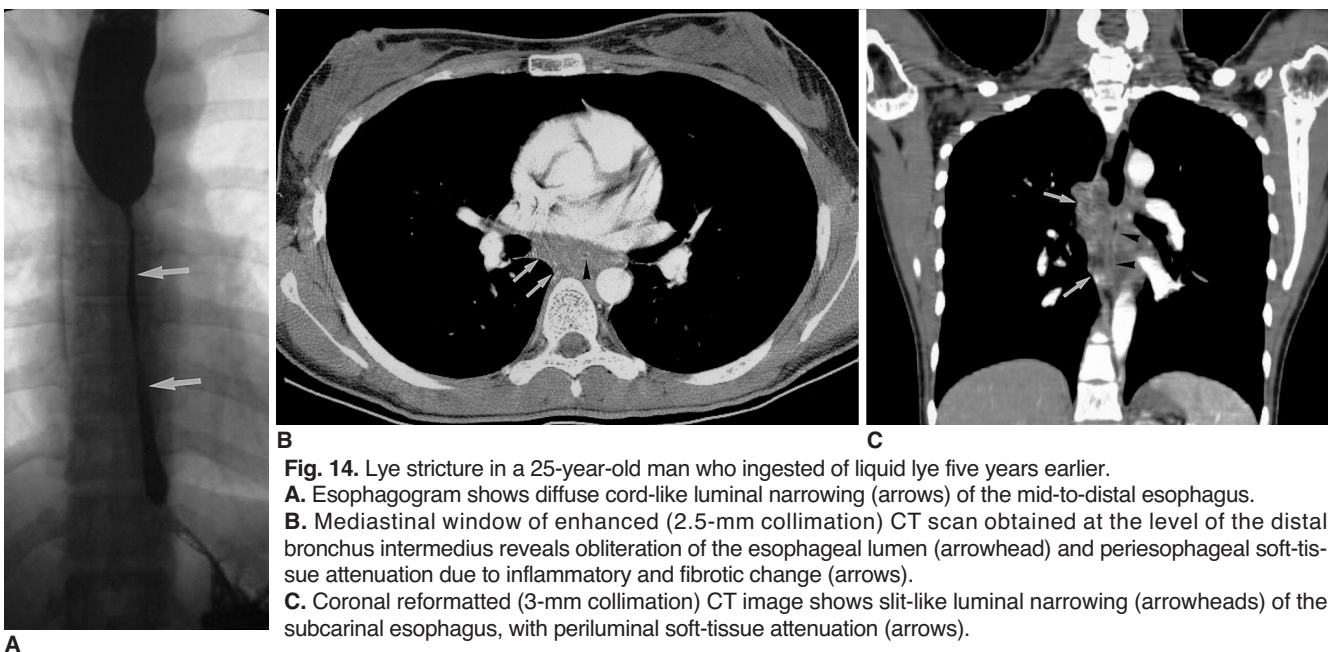
Fig. 14. Lye stricture in a 25-year-old man who ingested of liquid lye five years earlier.
A. Esophagogram shows diffuse cord-like luminal narrowing (arrows) of the mid-to-distal esophagus.
B. Mediastinal window of enhanced (2.5-mm collimation) CT scan obtained at the level of the distal bronchus intermedius reveals obliteration of the esophageal lumen (arrowhead) and periesophageal soft-tissue attenuation due to inflammatory and fibrotic change (arrows).
**C.** Coronal reformatted (3-mm collimation) CT image shows slit-like luminal narrowing (arrowheads) of the subcarinal esophagus, with periluminal soft-tissue attenuation (arrows).

tain no muscle, pulsion diverticula tend to remain filled after the esophagus has emptied of barium. When the esophagus collapses, traction diverticula tend to empty.

Esophageal Achalasia

Achalasia (megaesophagus) arises, in part, because relaxation at the lower esophageal sphincter level has failed to occur, and is partly due to the failure of organized peristal-sis. Among the various causes of dilatation of the esophagus, including achalasia, inflammatory stenosis, progressive systemic sclerosis (PSS) and carcinoma, achalasia causes the most severe generalized dilatation. Its symptoms include dysphasia, pain on swallowing, and chronic cough and recurrent pneumonia due to aspiration. Esophagography reveals, typically, that the lower end of the esophagus has a smooth, tapered, beak-like appearance at the level of
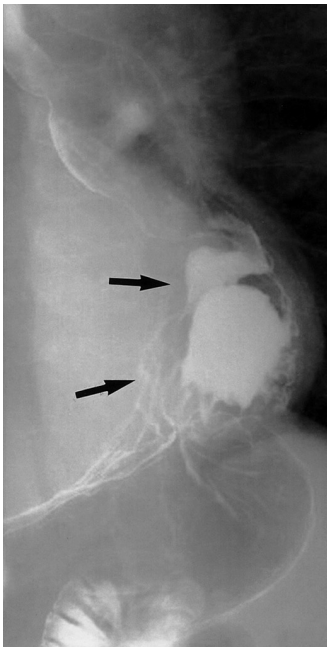
15A

15B
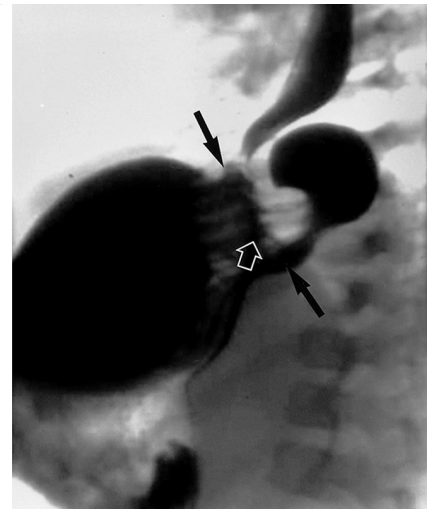
16

Fig. 15. Sliding hiatal hernia in a 30-year-old man.
A. Esophagogram shows that a portion of stomach (arrows) lies above the diaphragm.
B. Mediastinal window of enhanced (7-mm collimation) CT scan obtained at the level of the suprahepatic inferior vena cava shows that the thorax contains a portion of stomach (arrows). The aorta is displaced to the right.

Fig. 16. Paraesophageal hernia in a 2-year-old boy.
Esophagogram depicts elevated gastric fundus extending through the widened esophageal hiatus to the thoracic cavity (arrows). Note that the intra-abdominal position of the gastroesophageal junction (open arrow) is normal.
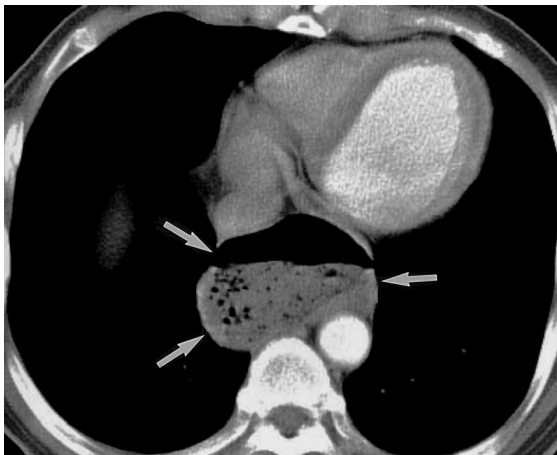
A

B

Fig. 17. Epiphrenic esophageal diverticulum in a 63-year-old man.
A. Mediastinal window of enhanced (7-mm collimation) CT scan obtained at the level of the suprahepatic inferior vena cava shows that outpouching (arrows) from the esophagus contains an air-fluid level.
B. CT scan obtained at the level of the liver dome shows that the position of the esophagogastric junction (arrow) is normal.

the esophageal hiatus (Fig. 18A). According to Rabushka et al. (30), who retrospectively reviewed the CT scans of nine achalasia patients, CT demonstrated moderate to marked esophageal dilatation (mean diameter : 4.35 cm at the carinal level), but normal wall thickness (Fig. 18B). Complications in patients with proven achalasia included pulmonary aspiration (three), secondary carcinoma (one), and iatrogenic esophageal perforation (one). It has been reported that secondary esophageal cancer develops in 2-7% of patients with longstanding achalasia (31). Routine CT may not be indicated, but in complicated cases may be in-

valuable in confirming the diagnosis or in detecting atypical features that may indicate the presence of other diseases or superimposed benign or malignant processes.

Esophageal and Paraesophageal Varices

In patients with underlying hepatic disease, the most common cause of esophageal and paraesophageal varices is portal hypertension, which leads to hepatofugal venous flow within esophageal or paraesophageal collateral vessels. Downhill varices associated with superior vena caval obstruction have also been reported (32). CT is useful in demonstrating the presence and extent of varices (33, 34) (Fig. 19), the appearance of which varies according to the severity and extent of the disease. At unenhanced CT, thickening of the esophageal walls may be visible, which enhanced CT reveals enhancing structures within the
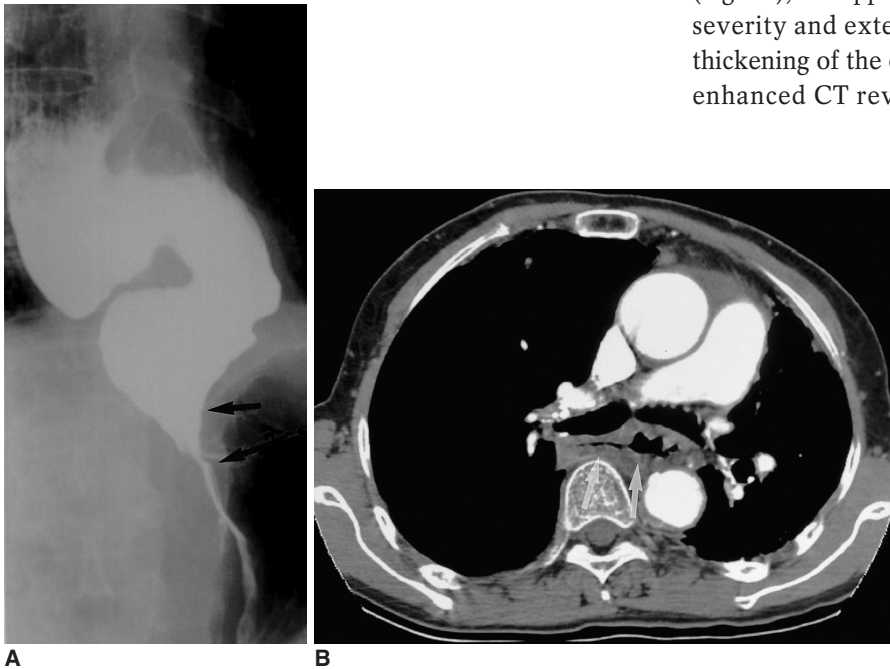
Fig. 18. Achalasia in a 50-year-old woman.
A. Esophagogram demonstrates smoothly tapered, beak-like narrowing at the esophagogastric junction (arrows) and a diffuse dilated esophagus.
B. Mediastinal window of enhanced (5-mm collimation) CT scan obtained at the level of the main bronchi shows a dilated esophagus (arrows), with mild diffuse wall thickening.
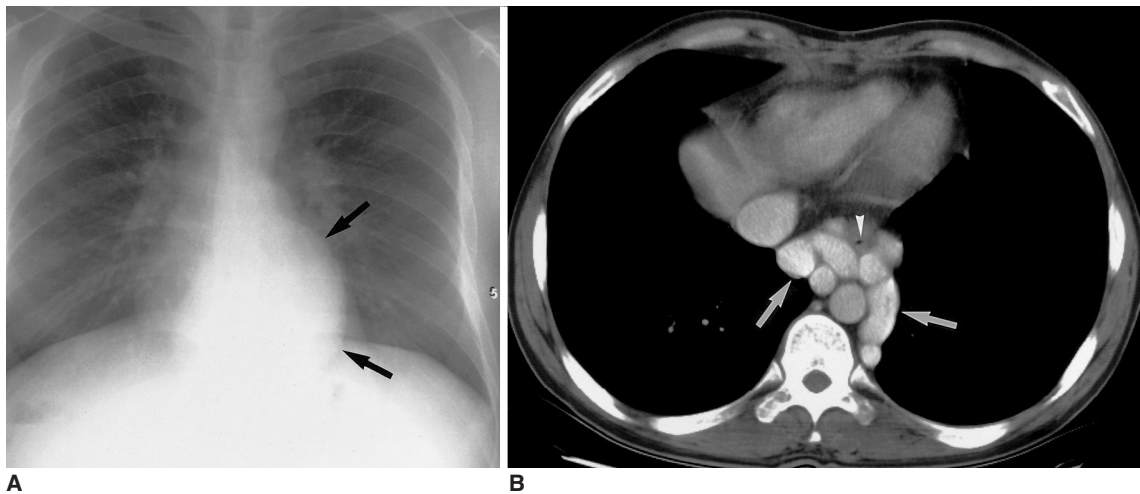
Fig. 19. Paraesophageal varices in a 45-year-old man with liver cirrhosis.
A. Chest radiograph depicts a retrocardiac soft-tissue mass (arrows).
B. Mediastinal window of enhanced (5-mm collimation) CT scan obtained at the level of the suprahepatic inferior vena cava shows enhancing tubular structures (arrows) surrounding the esophageal lumen (arrowhead).

esophageal wall or periesophageal region (33, 34).

CONCLUSION

The role of cross-sectional imaging in the evaluation of benign esophageal lesions continues to evolve. The advent of helical computed tomography and its volume data set facilitates the acquisition of multiplanar images; magnetic resonance imaging also helps acquire such images, as well as permitting tissue characterization. Through an awareness of the detailed morphology, location and extent of various benign esophageal lesions, as demonstrated by multiplanar cross - sectional imaging, the radiologist can play a more important role in the detection, diagnosis, and treatment of the diseases described in this paper.

References

1. Halber MD, Daffner RH, Thompson WM. CT of the esophagus: normal appearance. *AJR* 1979;133:1047-1050
2. Berkovich GY, Levine MS, Miller WT. CT findings in patients with esophagitis. *AJR* 2000;175:1431-1434
3. Seremetis MG, Lyons WS, DeGuzman VC, et al. Leiomyomata of the esophagus: an analysis of 838 cases. *Cancer* 1976;38:2166-2177
4. Cochat P, Guibaud P, Garcia Torres R, Roussel B, Guarner V, Larbre F. Diffuse leiomyomatosis in Alport syndrome. *J Pediatr* 1988; 113:339-343
5. Yang PS, Lee KS, Lee SJ, et al. Esophageal leiomyoma: radiologic findings in 12 patients. *Korean J Radiol* 2001; 2:132-137
6. Levine MS, Buck JL, Pantongrag-Brown L, Buetow PC, Hallman JR, Sobin LH. Fibrovascular polyps of the esophagus: clinical, radiographic, and pathologic findings in 16 patients. *AJR* 1996; 166:781-787
7. Cochet B, Hohl P, Sans M, et al. Asphyxia caused by laryngeal impaction of an esophageal polyp. *Arch Otoloaryngol* 1980; 106:176-178
8. Stoane JM, Torrisi JM, Haller JO, David M. Fibrovascular polyps of the esophagus: MRI findings. *J Comput Assist Tomogr* 1995; 19:157-159
9. Macpherson RI. Gastrointestinal tract duplications: clinical, pathologic, etiologic, and radiologic considerations. *RadioGraphics* 1993; 13:1063-1080
10. Kim YS, Park CK, Choi YW, Jeon SC, Seo HS, Hahm CK. Esophageal tubular duplication complicated by intraluminal hematoma: a case report. *J Korean Med Sci* 2000; 15:463-466
11. Kuhlman JE, Fishman EK, Wang KP, Siegelman SS. Esophageal duplication cyst: CT and transesophageal needle aspiration. *AJR* 1985; 145:531-532
12. Saito R, Kitamura M, Suzuki H, Ogawa J, Sageshima M. Esophageal schwannoma. *Ann Thorac Surg* 2000; 69:1947-1949
13. Ueyama T, Guo KJ, Hashimoto H, Daimaru Y, Enjoji M. Benign schwannoma of the gastrointestinal tract: a clinicopathologic and immunohistochemical study. *Hum Pathol* 1988; 19:257-264
14. Im J-G, Kim JH, Han MC, Kim CW. Computed tomography of esophagomediastinal fistula in tuberculous mediastinal lymphadenitis. *J Comput Assist Tomogr* 1990; 14:89-92
15. Levine MS, Macones AJ Jr, Laufer I. Candida esophagitis: accuracy of radiographic diagnosis. *Radiology* 1985; 154:581-587
16. Vahey TN, Maglinte DD, Chernish SM. State-of-the-art barium examination in opportunistic esophagitis. *Dig Dis Sci* 1986 ; 31:1192-1195
17. Graziani L, De Nigris E, Pesaresi A, Baldelli S, Dini L, Montesi A. Reflux esophagitis: radiologic-endoscopic correlation in 39 symptomatic cases. *Gastrointest Radiol* 1983; 8:1-6
18. Laufer I. Radiology of esophagitis. *Radiol Clin North Am* 1982 ; 20:687-699
19. Levine MS. Barrett's esophagus: a radiologic diagnosis? *AJR* 1988 ;151:433-438
20. Reid BJ. Barrett's esophagus and esophageal adenocarcinoma. *Gastroenterol Clin North Am* 1991; 20:817-834
21. Mori S, Yoshihira A, Kawamura H, Takeuchi A, Hashimoto T, Inaba G. Esophageal involvement in Behcet's disease. *Am J Gastroenterol* 1983; 78:548-553
22. Bhalla M, Silver RM, Shepard JO, McLoud TC. Chest CT in patients with scleroderma. *AJR* 1993; 161:269-272
23. Pasricha PJ, Fleischer DE, Kalloo AN. Endoscopic perforations of the upper digestive tract: a review of their pathogenesis, prevention, and management. *Gastroenterology* 1994; 106:787-802
24. Backer CL, LoCicero J , Hartz RS, Donaldson JS, Shields T. Computed tomography in patients with esophageal perforation. *Chest* 1990; 98:1078-1080
25. Berkman YM, Auh YH. CT diagnosis of acquired tracheoesophageal fistula in adults. *J Comput Assist Tomogr* 1985; 9:302-304
26. Wechsler RJ. CT of esophageal-pleural fistulae. *AJR* 1986; 147:907-909
27. Appelqvist P, Salmo M. Lye corrosion carcinoma of the esophagus: a review of 63 cases. *Cancer* 1980; 45:2655-2685
28. Lindell MM Jr, Bernardino ME. Diagnosis of hiatus hernia by computed tomography. *J Comput Assist Tomogr* 1981; 5:16-19
29. Kim KW, Berkmen YM, Auh YH, Kazam E. Diagnosis of epiphrenic esophageal diverticulum by computed tomography. *J Comput Assist Tomogr* 1988; 12:25-28
30. Rabushka LS, Fishman EK, Kuhlman JE. CT evaluation of achalasia. *J Comput Assist Tomogr* 1991; 15:434-439
31. Tishler JM, Shin MS, Stanley RJ, Koehler RE. CT of the thorax in patients with achalasia. *Dig Dis Sci* 1983; 28:692-697
32. Hirose J, Takashima T, Suzuki M, Matsui O. "Downhill" esophageal varices demonstrated by dynamic computed tomography. *J Comput Assist Tomogr* 1984; 8:1007-1009
33 Balthazar EJ, Naidich DP, Megibow AJ, Lefleur RS. CT evaluation of esophageal varices. *AJR* 1987; 148:131-135
34. Lee SJ, Lee KS, Kim SA, Kim TS, Hwang JH, Lim JH. Computed radiography of the chest in patients with paraesophageal varices: diagnostic accuracy and characteristic findings. *AJR* 1998; 170:1527-1531